UCRL-CONF-205448

LAWRENCE
LIVERMORE
NATIONAL
LABORATORY

Virtual Proving Ground for Assessing Reliability and Uncertainty

Henry Hsieh,
David Sam

30 July 2004

Foundation '04 V&V Workshop, Tempe, AZ, 13-15 October 2004

This work was performed under the auspices of the U.S. Department of Energy by University of California, Lawrence Livermore National Laboratory under Contract W-7405-Eng-48.

UCRL-CONF-205448

Virtual Proving Ground for Assessing Reliability and Uncertainty[1]

By

Henry Hsieh[2]
David Sam[3]

[1] This work was performed under the auspices of the U.S. Department of Energy by University of California, Lawrence Livermore National Laboratory under Contract W-7405-Eng-48.
[2] Structural and Applied Mechanics Group, New Technologies Engineering Division, Lawrence Livermore National Laboratory
[3] Advanced Engineering Analysis Group, Defense Technologies Engineering Division, Lawrence Livermore National Laboratory

ABSTRACT

The process for accurately estimating product reliability early in the development process can be a difficult and costly task. Traditional methods like Reliability Prediction Models and Life Testing Strategies yield beneficial results when relative information is known about the product that is to be analyzed. When there is minimal information (e.g., prior failure rates, etc.), such as in new concept design, these above reliability methods have limitations. For these cases computer simulation technology has proven to yield valuable results.

This paper will demonstrate analysis procedures for assessing the margin and reliability of product design in the early product development stage. This analysis process is composed of requirements definition, a mathematical model, model validation, parameter diagram, design of experiment (DOE), response surface, and optimization.

The analysis process shows its impacts, in the following areas: reducing the product development cycle, reducing cost, increasing confidence, and estimating product reliability. This is particularly important early in the concept development process.

Keywords: Computer Simulation, parameter variability, DYNA3D, Design of Experiments, Main Effect, Interaction Effect, Screening, Sensitivity Analysis, response surfaces

1. Introduction

To survive in today's intensely competitive business environment, most companies try to find new ways to increase profitability and to deliver high quality, reliable products. These goals could be achieved by using different strategies, such as shortening the product development cycle and minimizing resources, with varying degree of success. Computer simulation technology provides a promising and cost effective way to successfully implement these strategies.

Due to the rapid developments in computer simulation technologies, new analytical techniques are now available that include variability in the analysis procedure. In other words, some of the noise factors in the traditional parameter diagram can be analytically included in the analyses using computer simulation technology.

The Virtual Proving Ground (VPG) is an analytical process that enhances the traditional computer aided engineering (CAE) analysis process, which only analyzed the nominal designs. The enhancement is to incorporate variability into the analysis process. Its main purpose is to provide an estimate of the variability of product performance subjected to the influence of different sources of uncertainty.

Although it can and shall be implemented in every phase of the product development process, the Virtual Testing process shall be applied as early as possible to maximize its effects. In summary, VPG is an analytical process, which is developed to serve the following purposes:

- to improve the ability to explore, generate, and analyze different system attributes and structural design alternatives,
- to analytically account for the effects of variability in manufacturing and materials,
- to quantify the design risks, reliability, and sensitivity using probabilistic analysis tools and methods, and
- to optimize, if necessary, the product designs for selected performance parameters (such as cost, weight, design targets) over a range of variations of multi-attribute design parameters and constraints.

This paper is organized as follows: Section 2 briefly describes fundamentals of the analytical tools used to assess the margin and reliability. Section 3 describes an application example of the analysis procedure. This paper is closed with some conclusions in Section 4.

2. Analysis Procedure to Assess Margin and Uncertainty

Figure 1 shows the analysis procedure to assess margins and uncertainty. It consists of the following steps: Analytical Model, Parameter-Diagram (P-Diagram), Screening, Response Surface, Model Validation, and Margin and Reliability Assessment.

A complete understanding of the system requirements is necessary to successfully develop the analytical model. The requirements must be sufficiently defined to establish the scope of the problem, the goal of the analysis, and to identify necessary physics to be included.

2.1 Parameter Diagram

The first step in the analysis flowchart (Figure 1) is to identify each factor to be included in the parameter-diagram (Figure 2). This can only be done efficiently by reviewing the content of the analytical model and the nature of the application. During the course of the simulation analysis, certain assumptions are often made. Therefore, it is very important to review the content and the capability of the resultant analytical model in defining the P-diagram.

Figure 2 shows a typical P-Diagram. The term "control factor" is used to describe factors which can be controlled and affect the system response. Typical examples of control factors are: material selection, thickness, and design feature. The term "input factor" is used to describe the measurable, functional assumptions to which the system will respond. The "output factor" is the response of the system. The factors which can not be controlled are categorized as "noise factors". Here, we are concerned with 5 noise factors: (1) piece-to-piece interaction/ variation, (2) wear/fatigue, (3) product duty cycle, (4) environment (such as climate), and (5) systems interaction. Later in this paper, it will be demonstrated how to promote some of the noise factors to control factors through computer simulation techniques.

2.2 **Screening**

The central question of the screening experiment in the context of modeling and computer simulation is: which factors – among the many potentially important factors – are really important? One of the aims in modeling is to come up with a short list of important factors, and typically a risk-based graded approach is utilized to establish parameter hierarchy in terms of the importance of the system outcome. Screening methods are created to deal with models containing hundreds of input factors. For this reason, these methods must be economical. There exists a trade-off between computational cost and information obtained from these methods.

Some authors restrict the term ”screening designs” only to designs with fewer runs than factors (i.e. supersaturated designs). On the other hand, some authors speak of screening designs when the number of runs is larger than the number of factors. Myers and Montgomery[5] refer to fractional factorials being used as screening designs. In this report, the term screening refers to any preliminary activity that aims to identify which factors involved in a simulation model are most important. However, the fractional factorial method is applied for the screening experiment.

The purpose of screening is to search for k_1 factors that make significant effects on the objective response amongst the k_2 ($k_1 << k_2$) potentially important factors. This screening is needed if (1) the simulation study is still in its early, piloting phases, and (2) many factors may conceivably be important. A system with many factors will require many numerical simulations as well as computational resources. As an example, take the case in which there are N design factors. This requires (N+1) analyses to conduct first-order sensitivity analyses using a forward (backward or central) finite difference scheme. Computing the second order sensitivity matrix requires N(N-1)/2 analyses, in addition to the (N+1) analyses for first order analyses.

The computation cost of the experiment is defined as the number of simulations (or model evaluations) required. This cost is usually a function of the number of factors involved in the analysis and of the complexity of the input/output behavior.

The simplest class of screening designs is that of the one-at-a-time experiments (OAT). In these designs, the effect of each factor is evaluated in turn. In this report, we apply one particular OAT method, proposed by Cotter[6]. This screening design requires the following (2*k*+2) runs for *k* factors:

- one initial run with all factors at their low level;
- *k* runs with each factor in turn at its upper level, while all other k-1 factors remain at their low levels;
- *k* runs with each factor in turn at its low level, while all other factors remain at their upper level;
- one run with all factors at their upper level.

Denote the responses by $p_0, p_1, \cdots, p_k, p_{k+1}, \cdots, p_{2k}, p_{2k+1}$, then the order of importance for factor *j* can be assessed using the following equation:

$$M(j) = \left| \frac{(p_{2k+1} - p_{k+j}) + (p_j - p_0)}{4} \right| + \left| \frac{(p_{2k+1} - p_{k+j}) - (p_j - p_0)}{4} \right| .$$

One can then 'rank' the importance of each factor by comparing the value of *M(j)* between all the factors involved in the model. One major shortcoming of this method is that an importance factor may remain undetected. Another drawback is that it cannot provide information about interaction effects.

An alternate approach to the screening experiment is to use a factorial design scheme, in particular the fractional factorial design[5]. A $2^{\boldsymbol{k}}$ fractional factorial design containing 2^{k-p} runs is called a $\frac{1}{2^p}$ fraction of the 2^k design, or simply, a 2^{k-p} fractional factorial design. A 2^{k-p} fractional factorial design is of resolution IV if the main effects are clear of any two-factor interactions, but alias with three-factor interactions. If three-factors and higher interactions are suppressed, then the major effects may be estimated directly in a 2_{IV}^{k-p} design. For the screening experiment, one should start with a resolution IV design, if possible, since it differentiates the main effect from the three factors interaction effect.

2. 4 Response Surface

Consider a first-order polynomial, which is a model with only N main effects, besides the overall mean. By definition, a resolution III or R-3 design permits the unbiased estimation of such a first-order polynomial, which takes the form:

$$S_i = a_0 + \sum_{j=1}^{j=N} a_{j,i} x_j + \sum_{k=1}^{k=N} \sum_{j=1}^{j=N} b_{kj,j} x_k x_j + E_i \qquad (i = 1,2,3,\cdots n) \tag{1}$$

where

S_i : simulation response of factor combination *i*,

a_0 : overall mean response,

$a_{j,i}$:main effect of factor *j*,

$b_{kj,i}$: interaction effect of the factors *j* and *k*,

E_i : fitting error of the regression model for factor combination *i*,

n: number of simulation factor combinations.

It seems prudent to assume that interactions between pairs of factors (two-factor interactions) are important. By definition, a resolution IV or R-4 design permits the unbiased estimation of all *N* main effects, even if two-factor interactions are presented. However, R-4 designs do not give unbiased estimations of all N(N-1)/2 individual two-factors interactions. As compared with R-3 designs, R-4 designs require that the number of simulated two-factor combinations be doubled. For example, N=7 requires 8 and 16 simulations, respectively, for R-3 and R-4 designs. For the application example, which will be described in the next section, the "fold-over" principle was applied to construct the matrix for DOE analyses. In other words, the DOE matrix is established by creating the mirror image of the R-3 DOE matrix.

The central composite DOE (CCD) matrix, which considers a refined resolution of each factor is used, in conjunction with the preliminary DOE, to collect the data for our response surface model. The typical CCD consists of the following design points: (1) the axial point, which is the design point and (2) the center run. The axial points contribute in a large way to the estimation of quadratic terms. Without the axial points, only the sum of the quadratic terms, $\sum_{i=1,\ldots k} b_{ii}$, can be estimated. The axial points *do not* contribute to the estimation of the interaction terms. In general, the value of the axial distance varies from 1 to $\sqrt{k}$ where k is the number of design factors used in the CCD.

The center run provides an internal estimate of error (pure error) and contributes toward the estimation of quadratic terms. In the conventional DOE analyses, there are more than one center run to compensate for the inherent variation of the experiments. In the computer-simulation environment, there is no variation as long as the initial parameters/conditions do not change. Therefore, it is sufficient to use only one center run due to the nature of the computer simulation environment.

One can construct the response surface based on the results obtained from two sets of DOE (screening and central composite). The response surface model, equation (1), is called a multiple linear regression model with N regressor (or independent) variables. The method of least squares is typically used to estimate the regression coefficients.

2.5 Assessment of Margin and Reliability

After the response surface has been obtained, the margin and reliability of the design can be assessed through a variety of methods. The reliability, defined as the probability of the structure in safe state, is evaluated as follows:

$$R = \int_S p_X(x)dx = 1 - \int_F p_X(x)dx \qquad (2)$$

where $p_X(\cdot)$ is the joint probability density function of a random vector $X = (x_1, x_2, \cdots, x_n)$, S is the safe region, F denotes the failure domain, and the surface separating S and F is called the limit state function, $G(X)$. One can carry out the integration in equation (2) analytically.

However, this analytical approach can only be done for a very limited numbers of cases. For practical applications, which often involve random vectors with high dimensions, the analytical approach does not appear feasible. Numerical methods, such as Monte Carlo simulations, can generally be performed to evaluate the integration. The main drawback of such brute force evaluation is time-consuming. This is particular true when the computer simulation model is of large degree-of-freedom.

In this article, two methods are applied to assess the margin and reliability of the product. The first method is the first-order reliability method (FORM). The term "first-order" is used to describe that only the first-order expansion of the limit state function will be used for analysis. The term "second-moment" is used to refer that only the *mean* and *variation* of the design factors are required during the course of analysis. In the following, FORM will be briefly reviewed[2,10].

The basic idea in FORM is to approximate the failure surface by a single (or a set of) first order surface(s) and then calculate the failure probability using the approximate surface(s). In most of the applications of FORM, the problem is transformed into independent normal random variable space (also known as normalized space).

The center portion, which is the most challenging part, of reliability assessment is to find the location of the most probable point (MPP, or the checking point). The reliability index can be obtained after the location of the MPP has been identified. The first step in assessing the reliability is to transform the limit state function to normalized space. In other words, the design factors are transformed from the original random variables, $X = (x_1, x_2, \cdots, x_n)$, to Gaussian variables, $Z = (z_1, z_2, \cdots, z_n)$, with zero mean and unity variance. At the same time, the limit state function $G(X)$ will become $g(Z)$, where $Z = (z_1, z_2, \cdots, z_n)^T$ is a random vector. The MPP is the point in the normalized space that has the highest probability density function value on the limit state function $g(Z) = 0$ curve. The principle of variation will be applied to illustrate the concept. The search for the MPP is equivalent to minimizing the distance between the original and limit state function, which is expressed in terms of standard Gaussian random variables. With the introduction of Lagrange multiplier λ, the problem can be expressed as:

$$\min(L) = (Z^T \cdot Z)^{1/2} + \lambda \; g(Z) \quad . \tag{3}$$

For a stationary point, it is required that $\dfrac{\partial L}{\partial z_j} = 0$, for all j, which leads to

$$\frac{\partial L}{\partial z_j} = z_j (Z^T \cdot Z)^{-1/2} + \lambda \frac{\partial g}{\partial z_j} = 0\,, \tag{4}$$

and $\partial L / \partial \lambda = 0$ leads to $g(Z) = 0$ which is the limit state function itself. Now, the key is to solve for the location of the MPP using equation (4). From equation (4), one can solve for the co-ordinates for the stationary point, Z_s, as

$$Z_s = -\lambda\ \Delta_s \nabla g(Z_s) \tag{5}$$

in which the column vector

$$\nabla g(\cdot) = \left(\frac{\partial g}{\partial z_1}, \frac{\partial g}{\partial z_2}, \cdots, \frac{\partial g}{\partial z_n} \right)^T \tag{6}$$

stands for the gradient of the limit state function, and

$$\Delta = (Z^T \cdot Z)^{1/2} \tag{7}$$

denotes the distance between the point on the limit state function and the origin in the normalized space. One can solve for λ from equations (4) and (5). It turns out that

$$\lambda = \pm \frac{1}{\sqrt{\nabla g^T \cdot \nabla g}}\,, \tag{8}$$

where the sign is chosen so that equation (9) is always positive, and the resultant minimum distance Δ_s can be expressed as

$$\Delta_s = \pm \frac{-(Z_s)^T \cdot \nabla g}{(\nabla g^T \cdot \nabla g)^{1/2}} \geq 0\,. \tag{9}$$

The coordinates of the stationary point, which is the MPP, are

$$Z_s = \pm \frac{\Delta_s}{\sqrt{\nabla g^T \nabla g}} \nabla g \quad . \tag{10}$$

Again, the sign of equation (10) has to be consistent with equation (8). Equations (9) and (10) are the base for FORM. After the MPP has been located, the reliability index (RI) is given by

$$\text{RI} = \frac{E[G(X)]}{\sqrt{Var[G(X)]}} = \frac{E[g(Z_s)]}{\sqrt{Var[g(Z_s)]}} = \Phi(Z_s) \quad . \tag{11}$$

For a general limit state function which could be highly nonlinear, the search for the MPP is not an easy task. Here, a solution process based on an iterative solution scheme is introduced. Let $g(Z)$ be the general, nonlinear limit state function in normalized space. Let us consider the Taylor expansion of $g(Z)$ around $Z = Z_0$ which gives

$$g(Z) = g(Z_0) + \nabla g(Z_0)^T\ (Z - Z_0) + O(\|Z - Z_0\|^2) \tag{12}$$

Now, let us assume the search for the MPP will be convergent and ends when the error $O(\|Z - Z_0\|^2)$ reaches a pre-defined criterion. Under this circumstance, equation (12) can be expressed as

$$g(Z_{m+1}) = g(Z_m) + \nabla g(Z_0)^T \ (Z_{m+1} - Z_m) = 0 \tag{13}$$

where Z_{m+1} and Z_m stand for, respectively, the (m+1)-th and m-th approximation of the MPP. Equation (12) can be turned into a recurrence relationship:

$$Z_{m+1} = Z_m - \frac{g(Z_m)\,\nabla g(Z_m)}{\left(\nabla g(Z_m)^T, \nabla g(Z_m)\right)^{1/2}}. \tag{14}$$

Equation (14) can be used to obtain the location of the MPP. In practice, the iteration proceeds through the following steps:

1. Transfer the original design factors **X** to the independent standardized normal variables **Z**
2. Transfer the original limit state function G(**X**) to g(**Z**)
3. Select initial checking point Z_1
4. Compute the distance Δ_1 using equation (9)
5. Compute the normalized gradient function, $\frac{\nabla g(Z_m)}{\left(\nabla g(Z_m)^T \nabla g(Z_m)\right)}$ assuming m = 1
6. Compute Z_{m+1} using equation (13)
7. Check whether Z_m and Z_{m+1} have converged. If not, go back to step 5 and increase the index m by 1.

The second method, applied to analyze the reliability index, is Monte Carlo simulation. In the application example, the Monte Carlo simulation technique is applied to the resultant response surface directly. In other words, one assumes that the system response can be approximated, with reasonable accuracy, by an explicit function. One can then apply a Monte Carlo sampling scheme to study the response surface. The results from this Monte Carlo simulation include: mean, standard deviation, and distribution information of the system response.

3. Application Example

An encapsulated foam model is chosen as an example to illustrate the implementation of the analysis procedures described in Section 2. A layer of cellular foam with assumed material properties (stress versus strain curve, Figure 3) is put between two moldings. A preload is applied to the top molding. Along the material property curve, there is a region referred to as the lockup region. This lockup phenomenon is due to the nature of the cellular foam material being a porous material. As the foam is compressed, the pores begin to collapse until no pores remain. At this point, the compression response is governed by the bulk modulus of the dense material. On the plot of Figure 3 the lockup position is where the relatively flat curve abruptly transitions to the steep curve. Permanent deformation occurs when operation is within the lockup region. It is due to this, when the system reaches equilibrium, the maximal pressure is chosen to serve as the design criterion. The following assumptions are employed in assessing the margin and reliability:

- all design factors are assumed to be of Gaussian distribution,
- there exists some correlation between material properties in different regions, and
- the same correlation relation exists between foam thicknesses in different regions.

3.1 Model Description

The simulation model is chosen to be a very generic, versatile, hemispherical geometry. The model is depicted in Figure 4, and consists of the following components: rigid top molding, deformable top molding, rigid bottom molding, deformable bottom molding, and a layer of crushable (cellular) foam. To speed the computation, the top and bottom moldings are modeled as rigid bodies. Due to the big difference in material properties, particularly the Young's Modulus between the moldings and the cellular foam, the top and bottom rigid moldings are coated with one layer of deformable brick elements. Two sliding interfaces are placed to separate the cellular foam from the deformable top and bottom moldings. The bottom right molding is constrained in all 6 degree-of-freedoms whereas the top rigid molding is constrained along all of the rotational degree-of-freedom. The cellular foam layer is preloaded by applying a prescribed pressure to the top molding. To prevent being squeezed out from the molding, the top surface of the crushable foam is constrained along the translational y-direction.

The following factors are considered as primary candidates for sources of uncertainty: thickness of the foam, material properties of foam, preload of the system, sliding coefficient of friction of the interfaces (between foam and moldings), and the geometrical offset (mis-alignment) between the moldings. In real application, the material inhomogeneity, including properties and thickness, is a function of location. In reality, the thickness as well as material properties, of *every* brick element are sources of uncertainty. However, it is impractical and virtually impossible to include such uncertainties because of the enormous computational costs. Because of these concerns, the thickness (and material properties) of the foam are divided into 4 groups, as depicted in Figure 5. Three factors, x-offset, y-offset, and tilt-angle, are used to describe the geometrical uncertainties associated with the loading path of the top rigid molding. The coefficient of friction on the sliding interfaces are included as one source of uncertainty. Finally, the magnitude of the static preload is considered as one source of uncertainty. There are 13 design factors involved in the analysis: 4 for material properties, 4 for foam thickness, 3 for geometrical misalignment, 1 for coefficient of friction, and 1 for preload. These factors are summarized in Table 1.

3.2 Screening Experiment and Results

Because there are 13 design factors being included in the analysis procedure, a full two-level factorial design will require 2^{13} (=8192) runs. Instead of a full factorial design, only a fraction of these designs, which is equivalent to resolution IV design, are used in the screening experiments. Table 4 shows part (the first 48 cases) of the DOE matrix being used for the screening experiment. 128 simulation models were created based on the matrix and submitted for analyses. The resultant maximal pressure (hot spots) were collected and processed.

Figure 6 shows typical simulation results. Figures 7 and 8 show, respectively, the main effect and interaction effect plots from the screening experiment. After carefully studying these plots, the following conclusion can be drawn: (1) preload is the predominant factor, (2) foam thickness and properties are important factors, and (3) the coefficient of friction and geometrical misalignment do not have significant influence on the maximum response pressure. These observations were confirmed by the results from Cotter's screening design (Figure 9). Therefore, through the screening experiment, we identified 9 parameters which show significant influence over the system response. These are the parameters that were discussed in the previous section. We applied a central composite design scheme which consists of 19 designs: two designs for each parameter and one final design for the center point. The results from screening experiments and central composite design were collected and analyzed to obtain the response surface, an explicit function representing the functional relation between response and parameter. The resultant response surface of the system, expressed in terms of coded variables, appears as

$$R(X) = a_0 + b^T X + X^T CX$$

where $a_0 = 7.88$ is the constant term, b is the linear coefficient vector, C is the quadratic coefficient matrix. The values of b and C are provided in the appendix. We then move on to the next step, assessment of margin and reliability.

3.3 Assessment of Margin and Reliability

After the response surface of the system has been developed, we can assess the reliability of the system with a given design criterion. Let us assume the design criterion is that the maximal pressure is 9 MPa or less. Moreover, let us assume the following correlation matrix for both material properties and foam thickness:

$$Cov(X, X^T) = \sigma \begin{bmatrix} 1 & 0.3 & 0.03 & 0.3 \\ 0.3 & 1 & 0.3 & 0.03 \\ 0.03 & 0.3 & 1 & 0.3 \\ 0.3 & 0.03 & 0.3 & 1 \end{bmatrix} .$$

The limit state function, expressed in terms of coded variables, is convenient in developing the response surface and can be expressed as:

$$G(X) = (9 - a_0) - b^T X - X^T CX \ .$$

To assess the reliability using equation (11), we only need to calculate $E[G(X)]$ and $Var[G(X)]$. Using the values given in the Appendix, we calculate that $E[G(X)] = 1.12$ and $Var[G(X)] = 1.5838$. Therefore, the reliability index is RI=0.71 which corresponds to 76.7% of reliability.

The application of FORM to assess the MPP starts from expressing the limit state function in the normalized space. We assess the MPP using the iterative scheme as described in Section 2.4. Table 5 shows the iterative result in searching for the MPP.

The commercial software (Crystall Ball[4])[9] is applied to study the response of the system under the influence of random variables. Crystall Ball is a spreadsheet add-on that performs uncertainty analysis and creates graphic output for sensitivity analysis. It conducts Monte Carlo

[4] Crystal Ball is a registered trademark of Decisioneering, Inc.

simulation and risk analysis. Either simple Monte Carlo or Latin hypercube sampling schemes are available and can be used to simulate the outcome of a model. Figure 10 shows the simulation result using the Crystal Ball software. Figures 11 and 12 show, respectively, the contribution from linear and quadratic terms of the resultant response surface. Assuming the design criterion of maximal pressure (9 MPa or less) we can easily find that the corresponding reliability index and reliability are 0.71 and 76.70%, respectively.

4. Conclusion

An analysis process, consisting of concepts and methods from the following areas: (1) mathematical models, (2) model validation, (3) parameter diagram, (4) design of experiment, (5) response surface, and (6) optimization, has been presented in this article.

This analysis process shows how to incorporate noise factors into the analysis process. One example was used to demonstration its implementation to study the effect of piece-to-piece variation. Through a screening experiment, the process shows its capability to identify the significant design factors. It can also use to assess the reliability of the design. Optimization, which is not demonstrated explicitly in this example, can also be applied to improve the design.

The analysis process shows how it potentially impacts the following areas: reducing the product development cycle, reducing cost, and estimating product reliability (in particular, early in the product concept development process).

The analysis process can be extended easily to consider other application examples with different design criteria. Due to lack of experimental data, model validation - a very critical step - was not exercised. Model validation would enable us to quantify confidence bounds on the simulations[10] to complement the reliability methods described here[10]. A more rigorous procedure would start with a validated analytical model. The response surface should be developed within the application region. Another direction for future development would be to include other types of noise factors in the analysis. In the illustration example, we only considered the piece-to-piece variation effects. For future development, one could extend the analysis process to include other noise factors such environmental factors (temperature humidity) and component wear.

References:

1. Hsieh, Henry and Liddy, J., "A Virtual Testing Methodology for Automotive Concept Product Design", SAE 2002 SAE World Congress, March 4-7, Detroit, Michigan.
2. Melchers, R.E., *Structural Reliability: Analysis and Prediction*, John Wiley & Sons, Inc.
3. Montgomery, D. C., *Design and Analysis of Experiments*, John Wiley & Sons, Inc., 1991, ISBN: 0-471-52000-4.
4. Montgomery, D. C. and Peck, E. A., *Introduction to Linear Regression Analysis*, John Wiley & Sons, Inc., 1982, ISBN: 0-471-05850-5.
5. Myers, R. and Montgomery, D. C., *Response Surface Methodology: Process & Product Optimization Using Designed Experiments*, Wiley Series in Probability & Statistics, John Wiley & Sons, Inc., 1995, ISBN: 0471581003.
6. Kleijnen, J.P.C., Sensitivity Analysis and Related Analyses: A Review of Some Statistical Techniques, *Journal of Statistical Computation and Simulation*, 1997, Vol. 57, page 111-142,
7. Saltelli, A., Chan, K., and Scott, E. M. (editors), *Sensitivity Analysis*, John Wiley & Sons, 2000, ISBN 0-471-99892-3.
8. Shinozuka, M., Basic Analysis of Structural Safety, *Journal of Structural Engineering*, ASCE, Vol 109, No. 3, page 721-740.
9. Crystal Ball User Manual, Decisioneering, Inc., Denver Colorado, USA.
10. Nitta, C.K. and Logan, R.W., “Qualitative and Quantitative Linkages from V&V to Adequacy, Certification, Risk, and Benefit / Cost Ratio”, UCRL-TR-205809, Draft, July 2004.

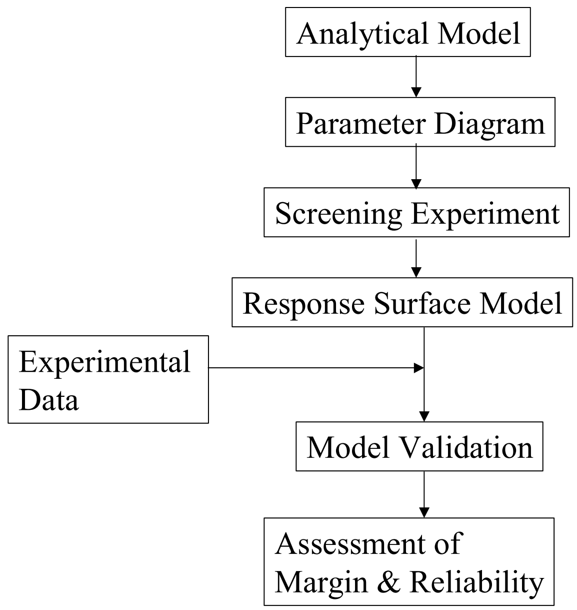

Figure 1: Analysis Flowchart

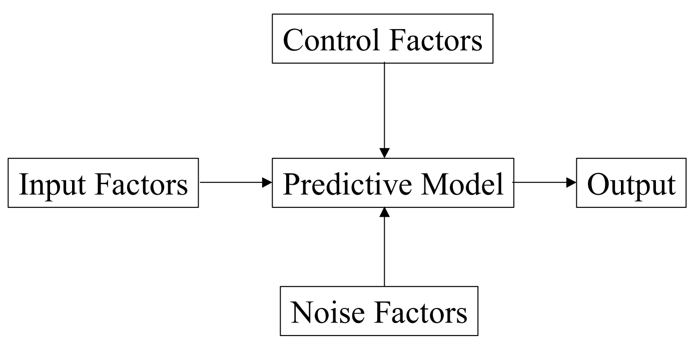

Figure 2: Parameter-Diagram

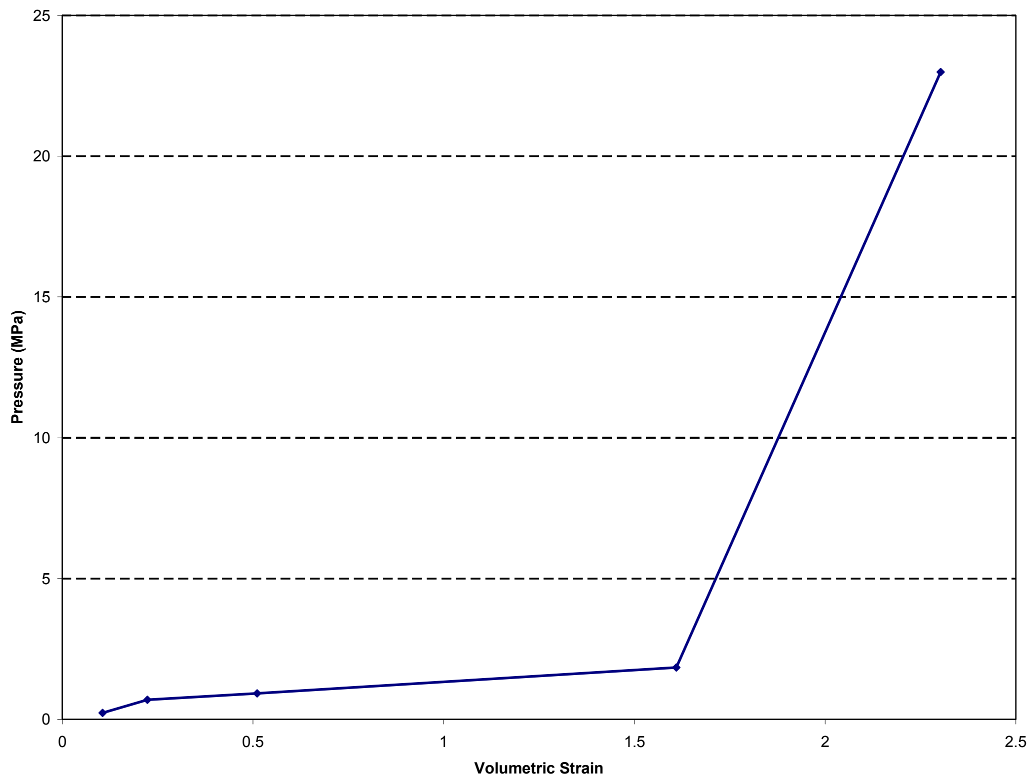

Figure 3: Material Property (Volumetric Strain versus Pressure Curve) for Cellular Foam

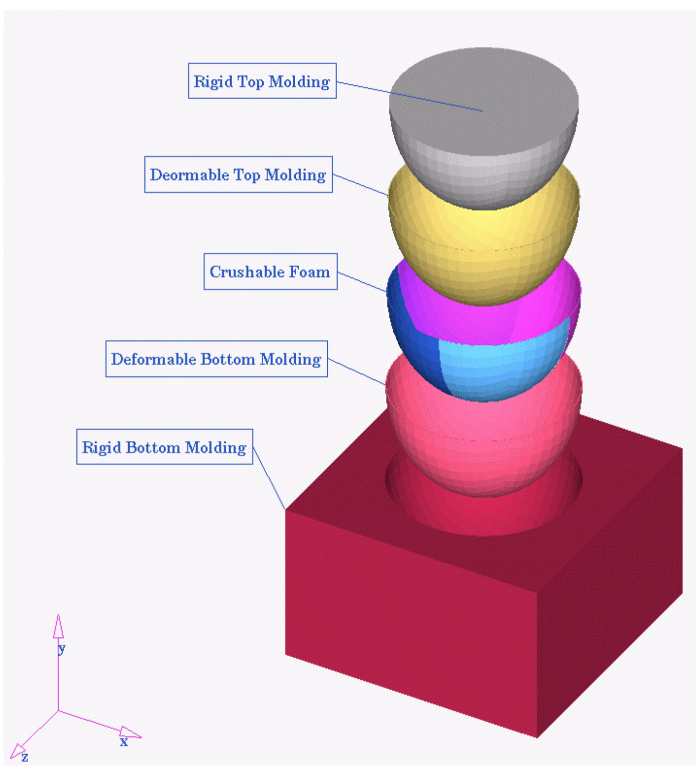

Figure 4: Layout of Simulation Model for generic hemispherical experiment.

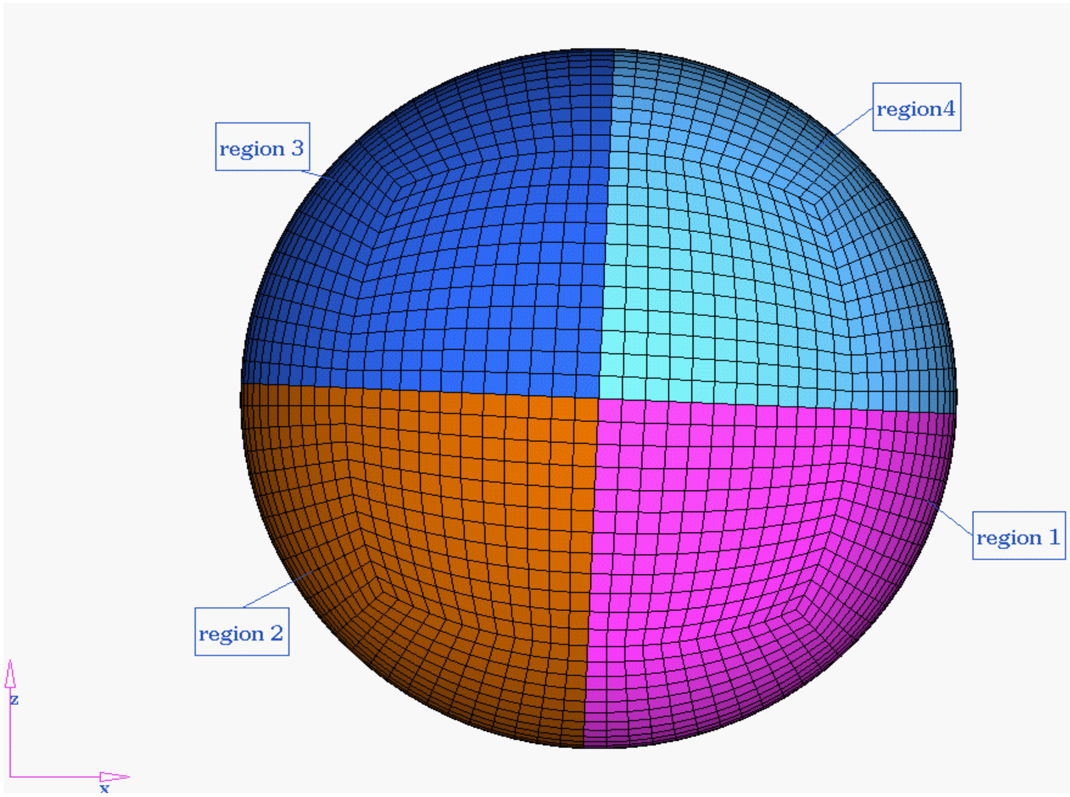

Figure 5: Layout of Cellular Foam

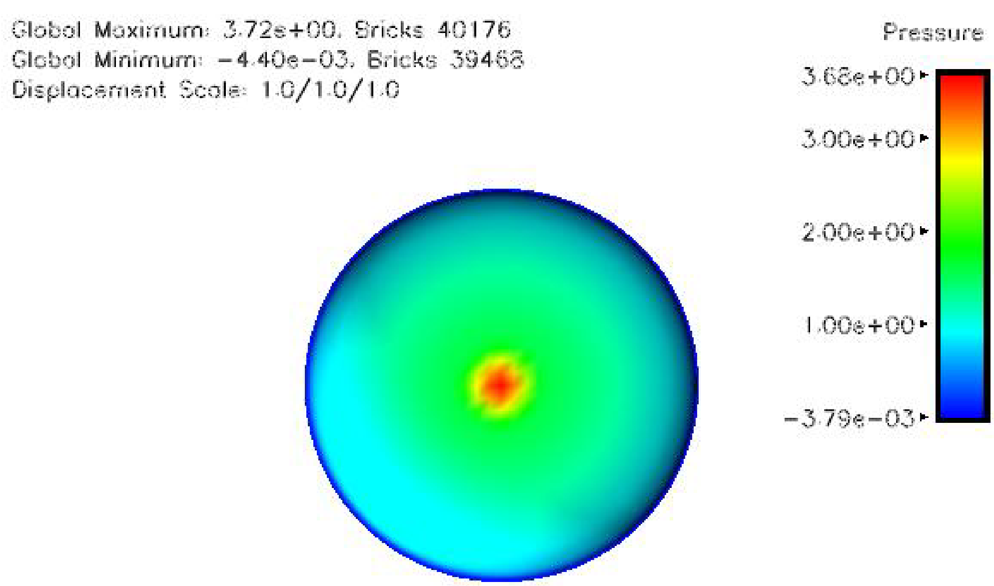

Figure 6: Typical response pressure distribution, t=2.

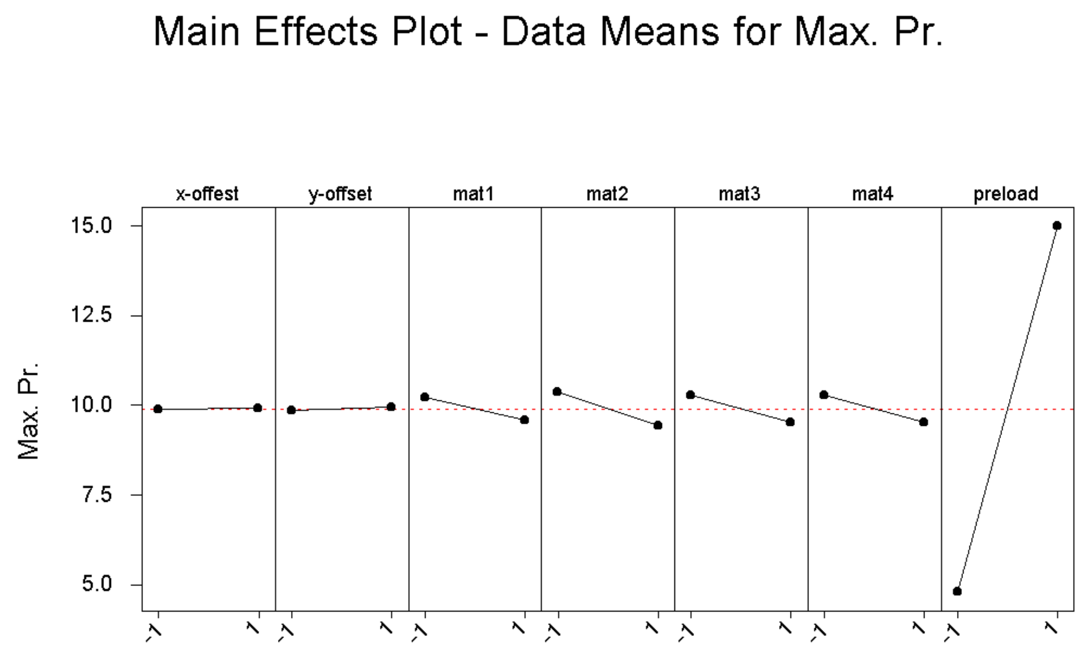

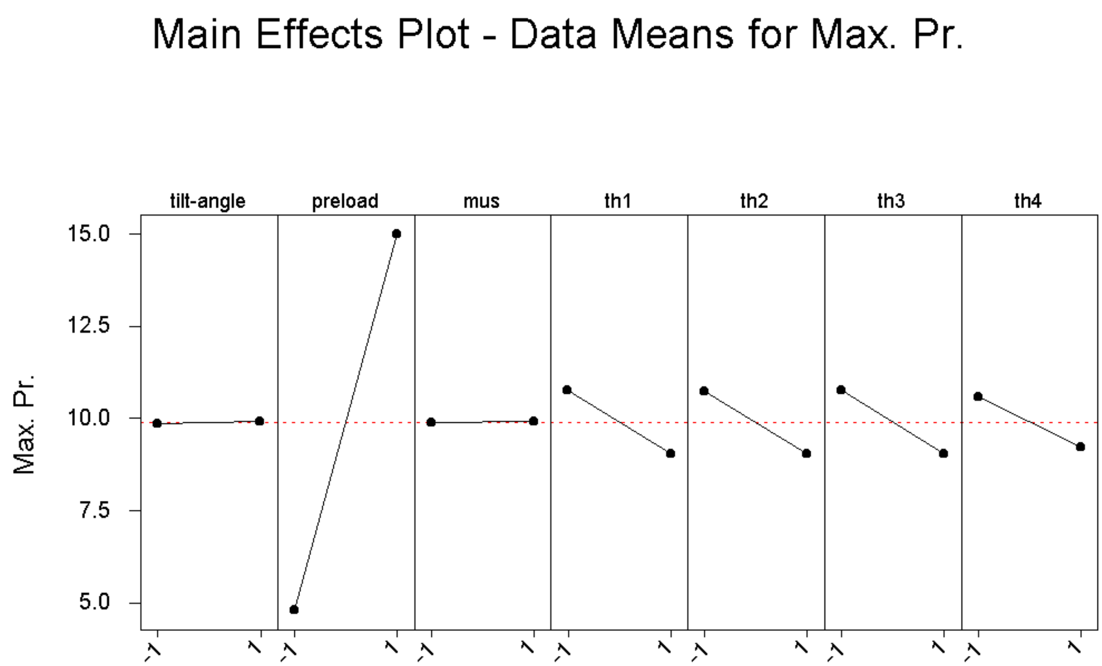

Figure 7: Main Effects Plots using Screen Experiment

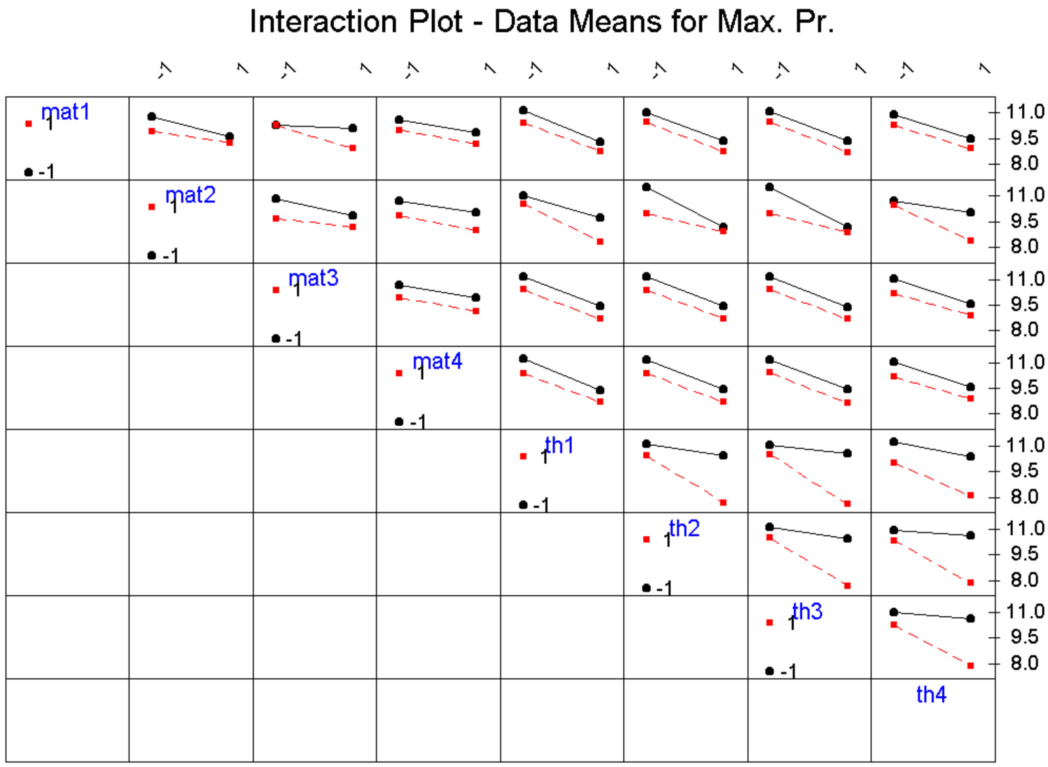

Figure 8: Interaction Plots using Screening Experiment

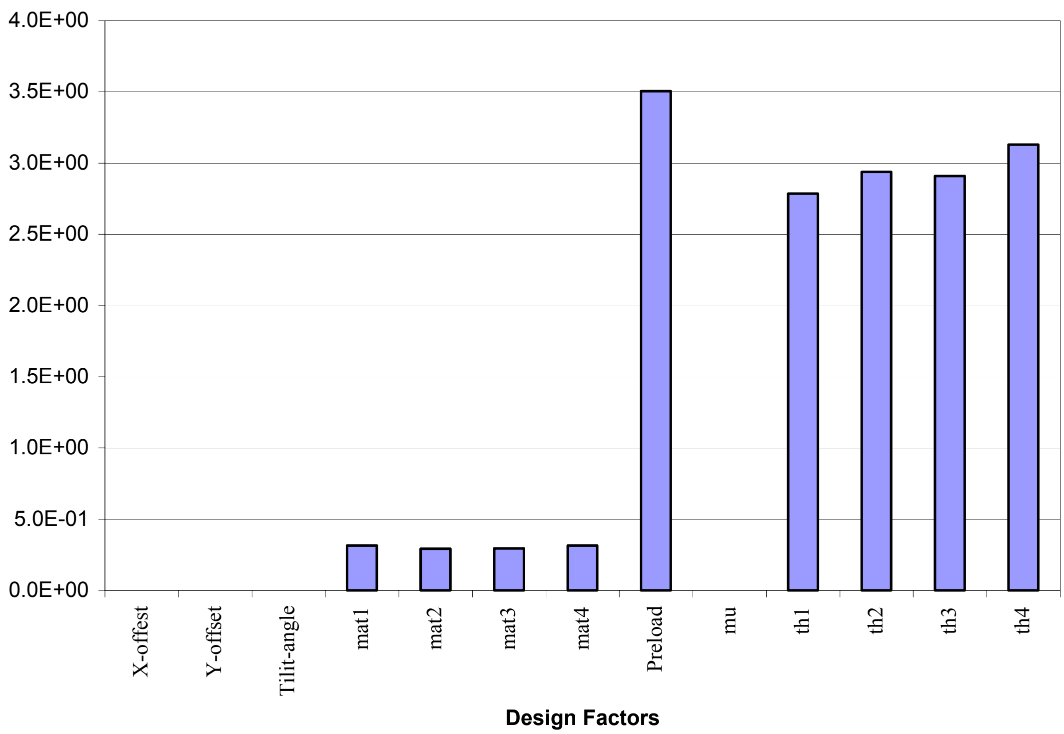

Figure 9: Order of Importance from Cotter's Design

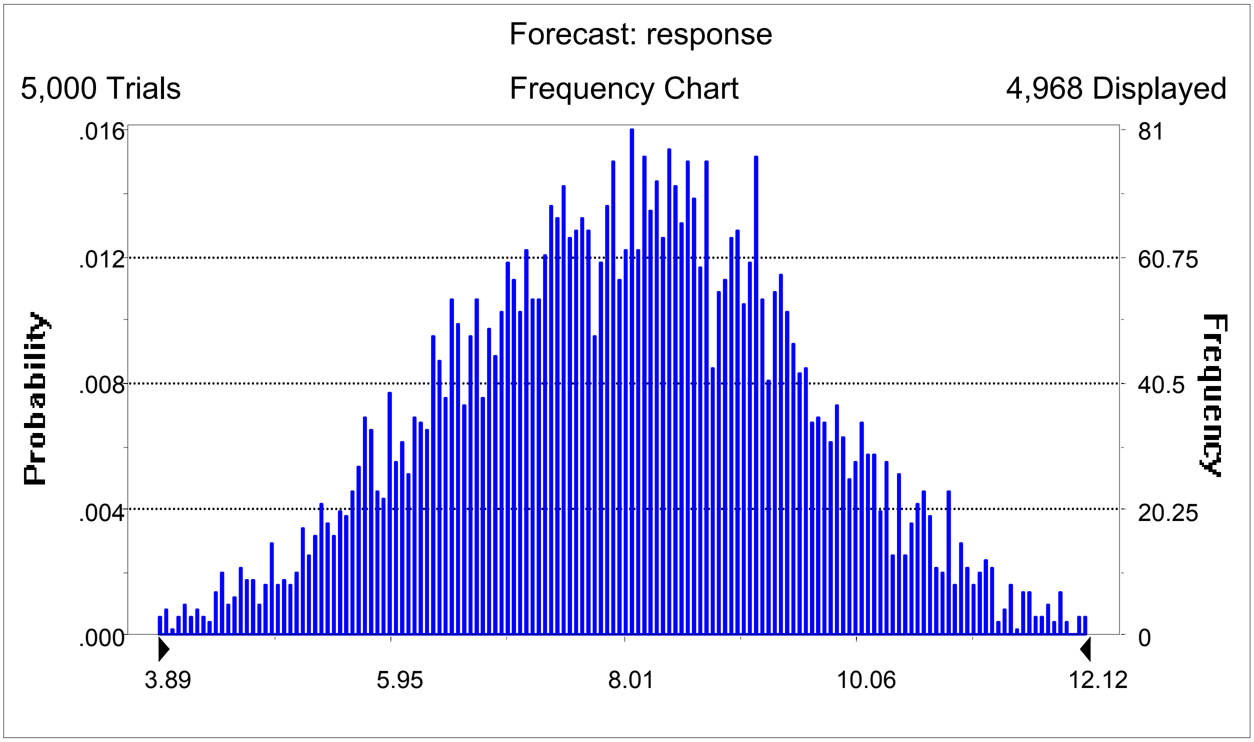

Figure 10: System Response from Monte Carlo Simulation

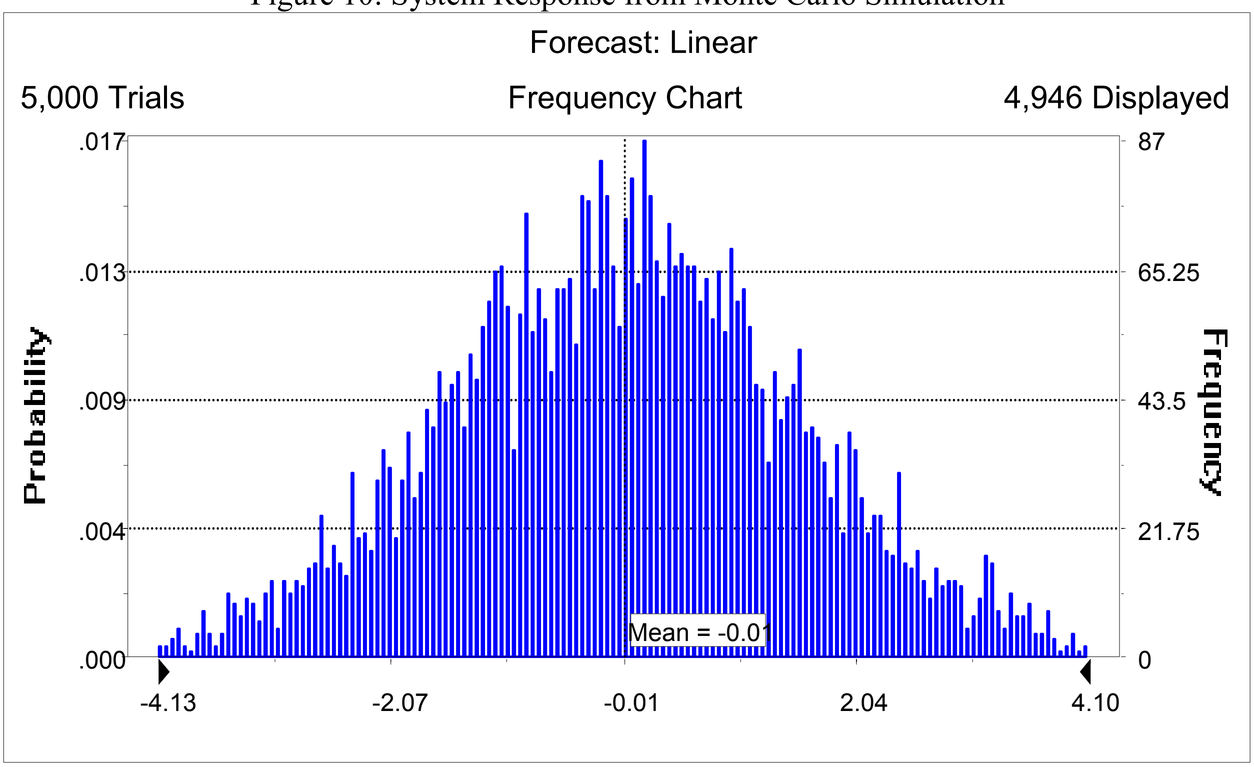

Figure 11: Contribution from Linear Term of Response Surface

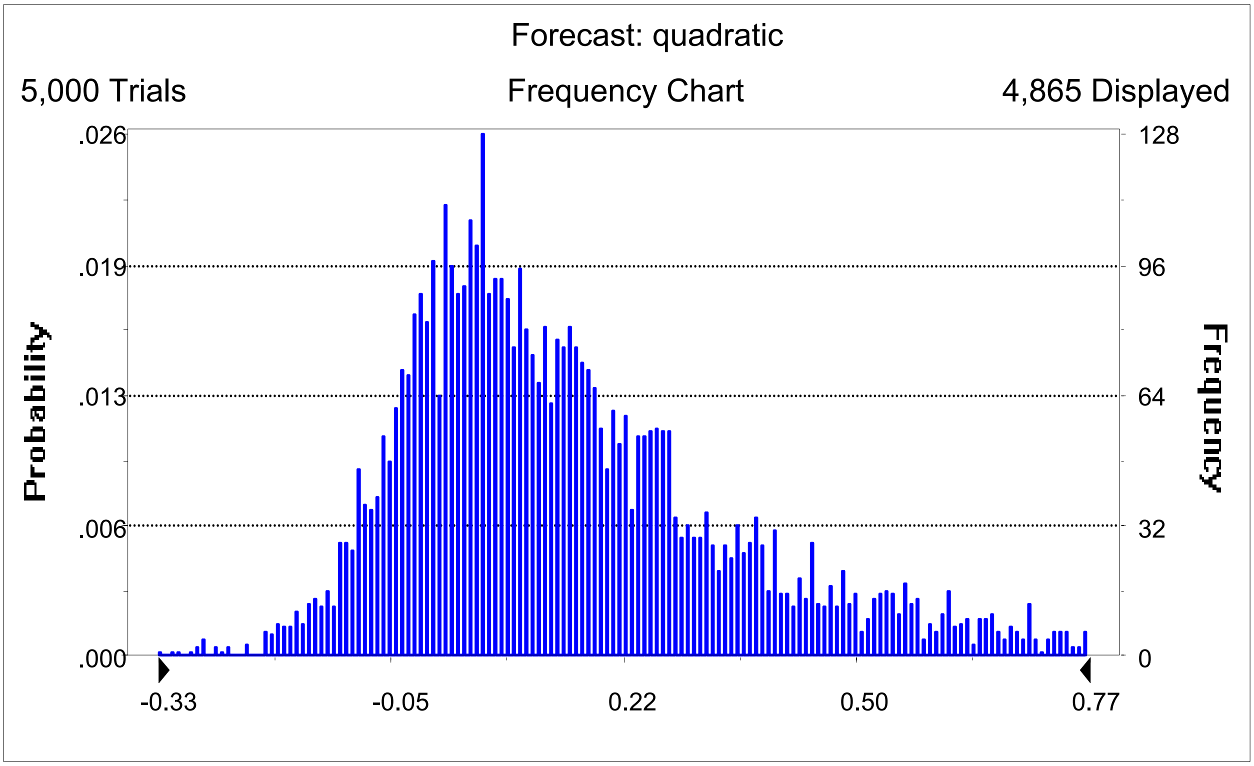

Figure 12: Contribution from Quadratic Terms of Response Surface

Table 1: List of Design Parameters

Design Parameter	Description
x-offset, z-offset	Geometrical mis-alignment (center line to center line) between the top and the bottom moldings
tilt-angle	Horizontal tilt angle of the top molding along z-direction
mat1, mat2, mat3, mat4	Material properties of cellular foam in different regions
preload	Magnitude of static preload being applied to system
mu	Static coefficient of friction used in the sliding interfaces
th1, th2, th3, th4	Thickness of cellular foam in different regions

Table 2: Relation between Coded and Natural Variables

Terms	Code Variable	Natural Variable				
		Symbol	Mean	Range	Standard Deviation	Transformation
x-offest	x_1	y_1	*0*	*0.635*	*0.106*	$x_1 = y_1 / 0.3125$
z-offest	x_2	y_2	*0*	*0.635*	*0.106*	$x_2 = y_2 / 0.3125$
tilt-angle	x_3	y_3	*0*	*1.0*	*0.167*	$x_3 = 2y_3$
mat1	x_4	y_4	*1.838*	*0.3676*	*0.0613*	$x_4 = (y_4 - 1.838)/0.1838$
mat2	x_5	y_5	*1.838*	*0.3676*	*0.0613*	$x_5 = (y_5 - 1.838)/0.1838$
mat3	x_6	y_6	*1.838*	*0.3676*	*0.0613*	$x_6 = (y_6 - 1.838)/0.1838$
mat4	x_7	y_7	*1.838*	*0.3676*	*0.0613*	$x_7 = (y_7 - 1.838)/0.1838$
preload	x_8	y_8	*1.75*	*0.50*	*0.083*	$x_8 = (y_8 - 1.75)/0.25$
mu	x_9	y_9	*0.40*	*0.08*	*0.013*	$x_9 = (y_9 - 0.40)/0.04$
th1	x_{10}	y_{10}	*6.35*	*0.635*	*0.106*	$x_{10} = (y_{10} - 6.35)/0.3125$
th2	x_{11}	y_{11}	*6.35*	*0.635*	*0.106*	$x_{11} = (y_{11} - 6.35)/0.3125$
th3	x_{12}	y_{12}	*6.35*	*0.635*	*0.106*	$x_{12} = (y_{12} - 6.35)/0.3125$
th4	x_{13}	y_{13}	*6.35*	*0.635*	*0.106*	$x_{13} = (y_{13} - 6.35)/0.3125$

Table 3: Cotter's One-At-A-Time Design

x-offset	z-offset	tilt-angle	mat1	mat2	mat3	mat4	preload	mu	th1	th2	th3	th4	response
-1	-1	-1	-1	-1	-1	-1	-1	-1	-1	-1	-1	-1	p0
+1	-1	-1	-1	-1	-1	-1	-1	-1	-1	-1	-1	-1	p1
-1	+1	-1	-1	-1	-1	-1	-1	-1	-1	-1	-1	-1	p2
-1	-1	+1	-1	-1	-1	-1	-1	-1	-1	-1	-1	-1	p3
-1	-1	-1	+1	-1	-1	-1	-1	-1	-1	-1	-1	-1	p4
-1	-1	-1	-1	+1	-1	-1	-1	-1	-1	-1	-1	-1	p5
-1	-1	-1	-1	-1	+1	-1	-1	-1	-1	-1	-1	-1	p6
-1	-1	-1	-1	-1	-1	+1	-1	-1	-1	-1	-1	-1	p7
-1	-1	-1	-1	-1	-1	-1	+1	-1	-1	-1	-1	-1	p8
-1	-1	-1	-1	-1	-1	-1	-1	+1	-1	-1	-1	-1	p9
-1	-1	-1	-1	-1	-1	-1	-1	-1	+1	-1	-1	-1	p10
-1	-1	-1	-1	-1	-1	-1	-1	-1	-1	+1	-1	-1	p11
-1	-1	-1	-1	-1	-1	-1	-1	-1	-1	-1	+1	-1	p12
-1	-1	-1	-1	-1	-1	-1	-1	-1	-1	-1	-1	+1	p13
-1	+1	+1	+1	+1	+1	+1	+1	+1	+1	+1	+1	+1	p14
+1	-1	+1	+1	+1	+1	+1	+1	+1	+1	+1	+1	+1	p15
+1	+1	-1	+1	+1	+1	+1	+1	+1	+1	+1	+1	+1	p16
+1	+1	+1	-1	+1	+1	+1	+1	+1	+1	+1	+1	+1	p17
+1	+1	+1	+1	-1	+1	+1	+1	+1	+1	+1	+1	+1	p18
+1	+1	+1	+1	+1	-1	+1	+1	+1	+1	+1	+1	+1	p19
+1	+1	+1	+1	+1	+1	-1	+1	+1	+1	+1	+1	+1	p20
+1	+1	+1	+1	+1	+1	+1	-1	+1	+1	+1	+1	+1	p21
+1	+1	+1	+1	+1	+1	+1	+1	-1	+1	+1	+1	+1	p22
+1	+1	+1	+1	+1	+1	+1	+1	+1	-1	+1	+1	+1	p23
+1	+1	+1	+1	+1	+1	+1	+1	+1	+1	-1	+1	+1	p24
+1	+1	+1	+1	+1	+1	+1	+1	+1	+1	+1	-1	+1	p25
+1	+1	+1	+1	+1	+1	+1	+1	+1	+1	+1	+1	-1	p26
+1	+1	+1	+1	+1	+1	+1	+1	+1	+1	+1	+1	+1	p27

Table 4: Factorial Design of Experiments Matrix used in Screening Experiments

case #	x-offset	y-offset	tilt-angle	mat1	mat2	mat3	mat4	preload	mu	th1	th2	th3	th4
1	-1	-1	-1	-1	-1	-1	-1	-1	1	1	1	1	1
2	1	-1	-1	-1	-1	-1	1	-1	1	1	-1	-1	1
3	-1	1	-1	-1	-1	-1	1	-1	-1	-1	-1	1	-1
4	1	1	-1	-1	-1	-1	-1	-1	-1	-1	1	-1	-1
5	-1	-1	1	-1	-1	-1	1	-1	-1	-1	1	-1	-1
6	1	-1	1	-1	-1	-1	-1	-1	-1	-1	-1	1	-1
7	-1	1	1	-1	-1	-1	-1	-1	1	1	-1	-1	1
8	1	1	1	-1	-1	-1	1	-1	1	1	1	1	1
9	-1	-1	-1	1	-1	-1	-1	1	-1	-1	1	1	1
10	1	-1	-1	1	-1	-1	1	1	-1	-1	-1	-1	1
11	-1	1	-1	1	-1	-1	1	1	1	1	-1	1	-1
12	1	1	-1	1	-1	-1	-1	1	1	1	1	-1	-1
13	-1	-1	1	1	-1	-1	1	1	1	1	1	-1	-1
14	1	-1	1	1	-1	-1	-1	1	1	1	-1	1	-1
15	-1	1	1	1	-1	-1	-1	1	-1	-1	-1	-1	1
16	1	1	1	1	-1	-1	1	1	-1	-1	1	1	1
17	-1	-1	-1	-1	1	-1	-1	1	1	-1	-1	-1	-1
18	1	-1	-1	-1	1	-1	1	1	1	-1	1	1	-1
19	-1	1	-1	-1	1	-1	1	1	-1	1	1	-1	1
20	1	1	-1	-1	1	-1	-1	1	-1	1	-1	1	1
21	-1	-1	1	-1	1	-1	1	1	-1	1	-1	1	1
22	1	-1	1	-1	1	-1	-1	1	-1	1	1	-1	1
23	-1	1	1	-1	1	-1	-1	1	1	-1	1	1	-1
24	1	1	1	-1	1	-1	1	1	1	-1	-1	-1	-1
25	-1	-1	-1	1	1	-1	-1	-1	-1	1	-1	-1	-1
26	1	-1	-1	1	1	-1	1	-1	-1	1	1	1	-1
27	-1	1	-1	1	1	-1	1	-1	1	-1	1	-1	1
28	1	1	-1	1	1	-1	-1	-1	1	-1	-1	1	1
29	-1	-1	1	1	1	-1	1	-1	1	-1	-1	1	1
30	1	-1	1	1	1	-1	-1	-1	1	-1	1	-1	1
31	-1	1	1	1	1	-1	-1	-1	-1	1	1	1	-1
32	1	1	1	1	1	-1	1	-1	-1	1	-1	-1	-1
33	-1	-1	-1	-1	-1	1	-1	1	-1	1	-1	-1	-1
34	1	-1	-1	-1	-1	1	1	1	-1	1	1	1	-1
35	-1	1	-1	-1	-1	1	1	1	1	-1	1	-1	1
36	1	1	-1	-1	-1	1	-1	1	1	-1	-1	1	1
37	-1	-1	1	-1	-1	1	1	1	1	-1	-1	1	1
38	1	-1	1	-1	-1	1	-1	1	1	-1	1	-1	1
39	-1	1	1	-1	-1	1	-1	1	-1	1	1	1	-1
40	1	1	1	-1	-1	1	1	1	-1	1	-1	-1	-1
41	-1	-1	-1	1	-1	1	-1	-1	1	-1	-1	-1	-1
42	1	-1	-1	1	-1	1	1	-1	1	-1	1	1	-1
43	-1	1	-1	1	-1	1	1	-1	-1	1	1	-1	1
44	1	1	-1	1	-1	1	-1	-1	-1	1	-1	1	1
45	-1	-1	1	1	-1	1	1	-1	-1	1	-1	1	1
46	1	-1	1	1	-1	1	-1	-1	-1	1	1	-1	1
47	-1	1	1	1	-1	1	-1	-1	1	-1	1	1	-1
48	1	1	1	1	-1	1	1	-1	1	-1	-1	-1	-1

Table 5: Iterative Result in Searching MPP

Parameter	0-th step	1-st step	2-nd step	3-rd step
x-offset	0.000	0.0037	0.0037	0.0037
z-offset	0.000	0.0213	0.0212	0.0212
tilt-angle	0.000	0.0134	0.0134	0.0134
mat1	0.000	-0.1257	-0.1252	-0.1252
mat2	0.000	-0.1815	-0.1807	-0.1807
mat3	0.000	-0.1495	-0.1489	-0.1489
mat4	0.000	-0.1557	-0.1551	-0.1551
preload	0.000	2.0449	2.0366	2.0366
mu	0.000	0.0081	0.008	0.008
th1	0.000	-0.1915	-0.1908	-0.1908
th2	0.000	-0.1692	-0.1685	-0.1685
th3	0.000	-0.1768	-0.1761	-0.1761
th4	0.000	-0.0886	-0.0882	-0.0882
residual error	-0.0046	-7.82E-08	1.26E-16	-9.89E-17

Appendix: Value of coefficient vector b and matrix C :

$$b = (0.008, 0.048, +0.030, -0.282, -0.406, -0.335, -0.349, 4.58, 0.018, -0.429, -0.379, -0.396, -0.198)$$

$$C = \begin{bmatrix} 0 & 0 & 0 & 0 & 0 & 0 & 0 & 0 & 0 & 0 & 0 & 0 & 0 \\ 0 & 0 & 0 & 0 & 0 & 0 & 0 & 0 & 0 & 0 & 0 & 0 & 0 \\ 0 & 0 & 0 & 0 & 0 & 0 & 0 & 0 & 0 & 0 & 0 & 0 & 0 \\ 0 & 0 & 0 & 0.013 & -0.003 & 0 & -0.006 & 0 & 0 & 0 & 0.008 & 0.007 & -0.001 \\ 0 & 0 & 0 & -0.003 & 0.012 & 0 & 0.006 & 0 & 0 & -0.002 & -0.02 & -0.02 & -0.001 \\ 0 & 0 & 0 & 0 & 0 & -0.002 & 0 & 0 & 0 & 0 & 0 & -0.002 & 0 \\ 0 & 0 & 0 & -0.006 & 0.006 & 0 & 0.029 & 0 & 0 & 0.002 & 0.015 & 0.011 & 0 \\ 0 & 0 & 0 & 0 & 0 & 0 & 0 & 0 & 0 & 0 & 0 & 0 & 0 \\ 0 & 0 & 0 & 0 & 0 & 0 & 0 & 0 & 0 & 0 & 0 & 0 & 0 \\ 0 & 0 & 0 & 0 & -0.002 & 0 & 0.002 & 0 & 0 & -0.038 & 0.006 & -0.008 & -0.003 \\ 0 & 0 & 0 & 0.008 & 0.019 & -0.001 & 0.015 & 0 & 0 & 0.006 & -0.109 & -0.013 & -0.015 \\ 0 & 0 & 0 & 0.007 & -0.016 & -0.002 & 0.011 & 0 & 0 & -0.008 & -0.013 & -0.105 & -0.009 \\ 0 & 0 & 0 & -0.001 & -0.001 & 0 & -0.004 & 0 & 0 & -0.003 & -0.015 & -0.009 & -0.005 \end{bmatrix}$$